Mode-locking of mobile discrete breathers

D. Zueco,[1,3,4] P. J. Martínez,[2,3,4] L. M. Floría,[1,3,4] and F. Falo[1,3,4]
[1]*Departamento de Física de la Materia Condensada, Universidad de Zaragoza, 50009 Zaragoza, Spain*
[2]*Departamento de Física Aplicada, Universidad de Zaragoza, 50009 Zaragoza, Spain*
[3]*Departamento de Teoría y Simulación de Sistemas Complejos. Instituto de Ciencia de Materiales de Aragón ICMA, C.S.I.C., Universidad de Zaragoza, 50009 Zaragoza, Spain*
[4]*Instituto de Biocomputación y Física de Sistemas Complejos BIFI, Universidad de Zaragoza, 50009 Zaragoza, Spain*
(Received 1 August 2003; published 18 March 2005)

We study numerically synchronization phenomena of mobile discrete breathers in dissipative nonlinear lattices periodically forced. When varying the driving intensity, the breather velocity generically locks at rational multiples of the driving frequency. In most cases, the locking plateau coincides with the linear stability domain of the resonant mobile breather and desynchronization occurs by the regular appearance of type-I intermittencies. However, some plateaus also show chaotic mobile breathers with locked velocity in the locking region. The addition of a small subharmonic driving tames the locked chaotic solution and enhances the stability of resonant mobile breathers.

DOI: 10.1103/PhysRevE.71.036613 PACS number(s): 05.45.Yv, 63.20.Pw

I. INTRODUCTION

Nonlinear lattices provide some of the most interesting model systems of macroscopic nonlinear behavior with experimental realizations [1]. From a theoretical perspective they have been progressively recognized not as mere discretizations of nonlinear continuous fields (unavoidable for numerical computations), but as a target of interest by themselves, due to the distinctive features associated with *discreteness*.

Among the variety of behaviors of the lattice nonlinear dynamics, we focus our attention here on the called "intrinsic localized modes" or "discrete breathers" (DB's). DB's are exact-periodic, large-amplitude, and exponentially localized solutions [2]. These solutions are made possible by the combination of nonlinearity and discreteness: Nonlinearity allows for solutions out of the linear mode bands, due to the frequency dependence of the oscillation amplitude. On the other hand, discreteness sets an upper cutoff in the band structure and prevents the multiharmonic resonances of DB's with extended linear modes. These two simple ingredients are enough for the existence of DB's, wherefrom the generality and wide range of interest of the phenomenon. To visualize an immobile DB see the upper part of Fig. 1.

These excitations are not only interesting from a theoretical point of view but with respect to the experimental applicability as well, concerning fields as diverse as biophysics (myelinated nerve fibers [1], biopolymer chains [3]), nonlinear optics (photonic crystals and waveguides [4]), Josephson effect (superconducting devices [5,6], Bose-Einstein condensates [7]) or the physics of glassiness [8]. This makes discrete breathers an object of remarkable multidisciplinary interest.

Unlike localization due to impurities or disorder (Anderson), intrinsic localization phenomena support mobile DB solutions—i.e., exponentially localized oscillations where the localization center propagates along the lattice as time goes by (see the lower part of Fig. 1). Although rigorous results apply to the generic existence of nonmoving DB's, much less is known about the conditions for their mobility. In this respect, Hamiltonian discrete breathers have received (comparatively) more attention than their dissipative counterparts. However, from the perspective of applications to experimental situations, the unavoidable coupling (both thermal and nonthermal) of the relevant degrees of freedom to a variety of other ones often demands one consider open systems where power balance, instead of energy conservation, governs the nonlinear dynamics of the lattice.

In this article we pay attention to the problem of synchronization and resonant behavior in *mobile* discrete breathers (MB's) of the forced and damped sine-Gordon lattice [the

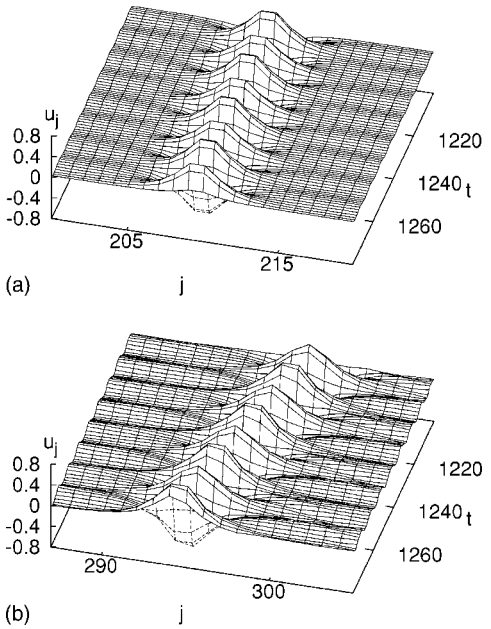

FIG. 1. Time evolution of two discrete breathers: (a) periodic pinned breather and (b) 1/2-resonant (see text) mobile breather. The localization center moves a lattice site every two periods of the external force.

one-dimensional (1D) standard Frenkel-Kontorova model [9–11]], illustrating the effects of *time scale competition* in breather dynamics, in a discrete, dissipative, and nonintegrable context. The two time scales of the moving pulse are, respectively, associated with its frequency ω_b and its velocity v_b. Our main results can be summarized as follows.

(i) Locking of the breather mean velocity at some rational values of the ratio $2\pi v_b/\omega_b$ for ranges of parameters (coupling, driving strength, etc.) is observable.

(ii) The synchronization of breather velocity is deeply rooted in the structural stability of pure resonant (to be defined soon) MB's, but it is by no means limited to it: The locking island in parameter space is generally larger than the linear stability domain of the pure resonant breather state.

(iii) The "extra" locking domain is characterized by more complex attracting breathers, sometimes chaotic in the breather core, but still keeping a locked velocity at large integration times.

(iv) When (sub)harmonic perturbations are added to the driving term, the stability of the pure resonant MB is enhanced (sometimes substantially), taming chaotic dynamics and enlarging the locking step size.

The paper is organized as follows: After this introductory section we present in Sec. II, in a brief but self-contained manner, the relevant and most basic aspects of dissipative breather mobility in the forced and damped discrete sine-Gordon equation (Frenkel-Kontorova model). The definition and characterization of (p/q)-resonant mobile DB's along with the extended Floquet method for the analysis of their linear stability are explained in this section.

In Sec. III we present our numerical results. We show that steps of the mode-locking velocity, where (p/q)-resonant solutions exist, are found when varying the driving strength. We see that this phenomenon is quite general since it is also found for an open set of coupling parameter values. In Sec. IV we focus our attention on the unlocking transition—i.e., the transition from (p/q)-resonant locking state to quasiperiodic (irrational $2\pi v_b/\omega_b$) generic velocity. This transition is characterized as a bifurcation via intermittencies of type I by using the Floquet methods reviewed in Sec. II. Section V is devoted to the phenomenon of locking enhancement by adding small additional subharmonic driving. Finally, some concluding remarks are given in Sec. VI.

II. MOBILE DB IN THE FRENKEL-KONTOROVA MODEL: RESONANT STATES AND THEIR STABILITY

Mobile dissipative discrete breathers have been well characterized [12] in the standard Frenkel-Kontorova (FK) chain subject to homogeneous periodic driving and viscous damping (see below). These solutions are *attractors* of the dynamics, and thus they are surrounded in phase space by a basin of attraction of initial conditions. This fact not only provides fast and accurate numerical methods for the continuation of generic mobile breathers (in contrast with expensive root finding methods for continuation in the Hamiltonian case), but also guarantees the very existence [13] of exact moving breathers (in contrast also with the Hamiltonian situation, where the stability and generality of exact moving solutions is currently an issue of debate [14]).

Generic MB's unavoidably excite extended modes (loosely referred to as phonons) which tend to delocalize energy. However, in dissipative systems, the locally excited phonons decay exponentially so that the mobile breather keeps on a finite localization length, essentially determined by the self-generated phonon dressing. The power spectrum (Fourier) analysis of the numerically exact MB's nicely validates their description as a moving source of damped radiation to the extent that the predictions of the theory exactly match the numerical spectra [15]. For resonant states (to be defined below) one can use Floquet methods in order to perform a more thorough analysis of these examples of exact nonintegrable mobility. This will become technically precise along this section, after explaining briefly the model and some relevant issues for the sake of self-containedness.

The equations of motion of the standard Frenkel-Kontorova model subject to a harmonic driving force $F_{ac}\sin(\omega_b t)$ and a viscous damping α are, in dimensionless form,

$$\ddot{u}_j + \alpha\dot{u}_j + \frac{1}{2\pi}\sin(2\pi u_j) = C(u_{j+1} - 2u_j + u_{j-1}) + F_{ac}\sin(\omega_b t), \tag{1}$$

where C denotes the coupling (indeed the coupling/nonlinearity ratio) between neighboring nonlinear oscillators $u_j(t)$ of unit mass.

Two different mechanisms for mobility of DB solutions of Eq. (1) have been observed.

(i) The spontaneous mirror symmetry breaking of pinned discrete breathers, which occurs at moderately low couplings, pave the way to mobility in a very natural manner, because a moving DB is a solution with broken symmetry. Indeed, this simple idea is at the origin of a very useful procedure [15–17] to prepare good initial conditions in the basin of attraction of exact mobile DB's: As described in detail elsewhere [12], adding a small perturbation (along the symmetry-breaking eigenvector, often dubbed as depinning mode) to the immobile exact DB often evolves asymptotically to an attracting moving solution.

(ii) Immobile quasiperiodic DB's have been seen to suffer from depinning parametric instabilities leading to mobile (typically slower) DB's [12] in a range of somewhat larger values of the coupling parameter. No stable pinned DB coexists in this range with moving solutions.

Once an attracting MB has been precisely determined, continuation from it through variations of parameters such as coupling or driving intensity generates a numerically continued branch of moving breathers. The continuation procedure of MB's from an initial one proceeds by a very small (adiabatic) change of a parameter—say, for example, ΔF_{ac} (or C or whichever)—and numerical integration during several periods (T_b) of the external driver. The convergence to the breather attractor corresponding to $F_{ac}+\Delta F_{ac}$ is guaranteed to be exponentially fast provided ΔF_{ac} is small enough and no bifurcation occurs.

The range of coupling values where these mobile solutions are observed is very far from the continuum regime; they are roughly in the range from $C=0.5$ to 1, and its mo-

tion has a well-defined average velocity. We should remark here that these MB's are not related to the breathers of the integrable (continuous) sine-Gordon model. The continuum limit of Eq. (1) is the continuous sine-Gordon equation under external ac forcing and losses, which does not support mobile breather solutions [18].

A convenient quantitative descriptor of a mobile localized solution is its translation velocity v_b. In order to define precisely this quantity, one has to introduce a continuous *collective variable* $X(t)$, naturally interpreted as the instantaneous center of localization of energy:

$$X = \frac{\sum_{j=-\infty}^{\infty} j \cdot \tilde{e}_j}{\sum_{j=-\infty}^{\infty} \tilde{e}_j}, \tag{2}$$

where $\tilde{e}_j = e_j - e_\infty$ is the energy density referred to the background, i.e.,

$$e_j = \frac{1}{2}\dot{u}_j^2 + \frac{1}{(2\pi)^2}[1 - \cos(2\pi u_j)] + \frac{C}{4}(u_j - u_{j-1})^2 + \frac{C}{4}(u_{j+1} - u_j)^2, \tag{3}$$

and e_∞ is e_j at a site j far away from the exponentially localized breather core. The breather velocity is then defined as the following long-term average velocity:

$$v_b = \langle \dot{X} \rangle = \lim_{T\to\infty} \frac{1}{T} \int_{t_0}^{t_0+T} \dot{X}\, dt. \tag{4}$$

Along a single branch of continued MB's, the breather velocity defines a continuous *but not necessarily smooth* curve. Let us emphasize that moving solutions of velocity v_b possess two characteristic time scales: namely, ω_b and $2\pi v_b$. The issue of time scale competition is thus of concern here, in the sense that one would naturally expect the emergence of typically associated phenomena, like resonances and synchronization in the behavior of MB's, as demonstrated by numerical results to be shown later in Sec. III. Now let us introduce some basic notions needed for what follows.

A. Resonant mobile discrete breathers

A close view of Eq. (1) reveals the basic symmetries of the dynamics.

(a) Lattice translation (homogeneous system)

$$\mathcal{L}\{u_j(t)\} = \{u_{j+1}(t)\}. \tag{5}$$

(b) Discrete time T_b shift (periodic driver)

$$\mathcal{T}\{u_j(t)\} = \{u_j(t + T_b)\}. \tag{6}$$

(c) Space-time mirror symmetry (specific to such situations)

$$\mathcal{S}\{u_j(t)\} = \left\{ -u_j\left(t + \frac{1}{2}T_b\right)\right\}. \tag{7}$$

This operator combines the mirror symmetry $\mathcal{R}(u) = -u$ of the local term $\sin(u)$ and the center symmetry of the sinusoidal driver: $\mathcal{S} = \mathcal{R}\mathcal{T}^{1/2}$.

Given any solution $\{\hat{u}_n(t)\}$, the combined action of the symmetry operators $\mathcal{L}$, $\mathcal{T}$, and $\mathcal{S}$ gives a family of solutions generated by the symmetry group. We will see that the existence and structure of this family play a central role in our interpretation of numerical results on desynchronization of moving DB's.

Now we will make precise the notion of resonant DB, used in the Introduction. A (p/q)-resonant state is a synchronized orbit defined as fixed point of the symmetry element $\mathcal{L}^p\mathcal{T}^q$, i.e.,

$$\hat{u}_{n+p}(t + qT_b) = \hat{u}_n(t). \tag{8}$$

If p and q have no common divisors, the state is said *pure resonant*. Note that it follows from the definition that a (p/q)-resonant MB has a velocity $v_b = (\omega_b/2\pi)(p/q)$. But it is also important to realize that among all conceivable evolutions $\{u_n(t)\}$ with this velocity, a resonant one is certainly very special, for it possesses a specific $(\mathcal{L}^p\mathcal{T}^q)$ symmetry.

B. Linear stability analysis

Let us consider a small perturbation $\{\epsilon_j(t), \dot{\epsilon}_j(t)\}$ of a given DB solution $\{u_j(t)\}$. Linearizing around this solution, we obtain

$$\ddot{\epsilon}_j + \alpha\dot{\epsilon}_j + \cos[2\pi u_j(t)]\epsilon_j = C(\epsilon_{j+1} - 2\epsilon_j + \epsilon_{j-1}). \tag{9}$$

An immobile DB of frequency ω_b is a fixed point of the operator $\mathcal{T}$. The *Floquet* matrix maps a basis of the tangent space $(\{\epsilon_j(0), \dot{\epsilon}_j(0)\})$, onto $\{\epsilon_j(T_b), \dot{\epsilon}_j(T_b)\}$, and it is given by the Jacobian of $\mathcal{T}$—i.e., $D(\mathcal{T})$. The spectrum of eigenvalues of this Floquet matrix gives the linear stability of immobile DB's, allowing the characterization of the bifurcations that these solutions experience along continuation paths, as shown in Refs. [12,15]. In order to use these powerful Floquet methods for the analysis of mobile solutions, they must be periodic, and so one has to restrict attention to (p/q)-resonant MB's.

Because a (p/q)-resonant MB is a fixed point of the operator $\mathcal{L}^p\mathcal{T}^q$, the (extended) Floquet matrix providing the linear stability of a (p/q)-resonant MB is $D(\mathcal{L}^p\mathcal{T}^q) = \mathcal{P}\mathcal{M}$, where $\mathcal{M}$ is the matrix of the linearized equations of motion integrated over q T_b periods and (periodic boundary conditions) $\mathcal{P}$ is a cyclic permutation matrix of p sites:

$$\{\hat{u}_j(t_0) + \epsilon_j(t_0), \hat{u}_j(t_0) + \dot{\epsilon}_j(t_0)\} \to \{\hat{u}_j(t_0), \hat{u}_j(t_0)\} + \mathcal{P}\mathcal{M}\{\epsilon_j(t_0), \dot{\epsilon}_j(t_0)\}. \tag{10}$$

The distinctive property of being an attracting solution of the nonlinear evolution equation (1) translates into the mathematical assertion that an attracting (p/q)-resonant state has an associated Jacobian matrix $D(\mathcal{L}^p\mathcal{T}^q)$ with (bounded) spectrum inside the complex unit circle:

$$\sup|\mu| \leqslant 1, \tag{11}$$

where μ denotes eigenvalues of the Floquet matrix.

Eventually, the exit of a Floquet eigenvalue from the unit circle signals the destabilization of the (p/q)-resonant MB

by perturbations along the associated Floquet eigenvector. In the linear regime these destabilitations will grow with an exponential rate.

III. INTERNAL STRUCTURE OF THE LOCKING REGIME

First of all, we briefly review the method used to generate mobile discrete breathers. We begin by generating an immobile discrete breather, starting from the anticontinuum limit ($C=0$). Initially, we have used the same parameters as in [15]: $F_{ac}=0.02$, $\omega_b=0.1\times 2\pi$, and $\alpha=0.02$. As we increase C adiabatically, the discrete breather solution remains as an attractor of the dynamics [15], enabling us to find breathers at different values of C, by continuation.

We continue the breathers until the first pitchfork bifurcation [15–17], which connects one-site breathers with two-site breathers via asymmetric ones. The localized eigenmode, responsible for this instability, is asymmetric and can be used to "depin" the static breather. Then, we generate a MB by perturbing the static breathers along this mode with an amplitude μ. As in [15,16], we found MB's if the perturbation is larger than some critical value μ_c. Unlike Hamiltonian systems, the velocity reached by the MB is independent of μ for $\mu>\mu_c$. This method allows us to produce MB's in a wide range of the coupling parameter C. Two kinds of MB's have been observed depending on C: for C in the interval [0.5, 0.89] only induced MB's exist in coexistence with static breathers. However, in the C range [0.89, 0.97] spontaneous MB's appear as attractor solutions, coexisting whith the induced MB's. Static breathers are not found in this range. Hence, we have decided to focus our research on some points in those regions. The selected values are $C=0.55$ and $C=0.75$ in the first region and $C=0.94$ in the second.

In order to check the dependence of these MB's on the driving force, we fix C and then we vary F_{ac}. Some general features emerge in all cases. The simulations show the appearance of steps with velocities $v_b=(\omega_b/2\pi)(p/q)$. Recall that these velocities are the velocities of mode-locked MB's. But this does not guarantee that the MB inside the locking step is (p/q) resonant, so we must check the periodicity of these MB's inside these steps. Another empirical observation is that the limit value of F_{ac} before the destruction of the MB increases with C.

The results with $C=0.55$ are sketched in Fig. 2. This figure shows the full F_{ac} range in which MB's with a definite velocity exist. One can see an extremely narrow step at velocity $v_b=(\omega_b/2\pi)(1/3)$. The Poincaré section of these solutions reveals that they are *pure resonant MB's*. Moreover, the linear stability analysis reveals that they are linearly stable inside the whole step interval—i.e., $[0.01568,0.01581]_{F_{ac}}$. This type of solution, i.e. $(1/3)$-resonant, has been found in the whole range of C values that we investigated.

For $C=0.75$, the results of the velocity-force curve are represented in Fig. 3. In this case we find a bigger step at velocity $v_b=(\omega_b/2\pi)(1/2)$ ($[0.03177,0.042]_{F_{ac}}$) and, again, a very little one at $v_b=(\omega_b/2\pi)(1/3)$ ($[0.01534,0.01538]_{F_{ac}}$). In the whole interval of this last step, the MB is $(1/3)$ resonant and linearly stable. On the other hand, the bigger step has a more complex structure: In the range $[0.03177,0.03831]_{F_{ac}}$, the MB is periodic with period $2T_b$ and linearly stable. These $(1/2)$-resonant solutions can be continued in coupling parameters from $C\simeq 0.71$ up to $C\simeq 0.84$. However, at $F_{ac}\simeq 0.03831$ the MB suffers a transition of period tripling (a Floquet eigenvalue and its complex conjugate cross the unit circle at angles $2\pi/3$ and $-2\pi/3$) and rapidly goes to a chaotic state via a *period-doubling cascade* for $F_{ac}\simeq 0.03833$. The MB remains in this chaotic state with commensurate velocity, and around $F_{ac}\simeq 0.042$, the solution leaves the step.

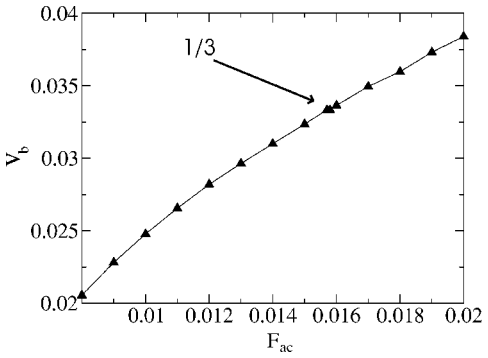

FIG. 2. Velocity of the MB vs F_{ac} for $C=0.55$. A very narrow plateau $\frac{1}{3}$ appears. The rest of fixed parameters are $\omega_b=0.1\times 2\pi$ and $\alpha=0.02$.

Finally, at $C=0.94$ we obtain the curves represented in the Fig. 4. There we can observe a very rich behavior of the breather velocity: different steps at velocity values of $(\omega_b/2\pi)(1/3)$, $(\omega_b/2\pi)(4/9)$, and $(\omega_b/2\pi)(2/3)$, as well as an evident hysteresis. The latter is somehow typical of underdamped systems; it implies the coexistence of (at least) two different MB attractors, with the same model parameters which has been reported previously [15,19]. The dynamics in these steps is simple: periodic and linearly stable, with no bifurcations inside the plateau. Also a smaller plateau with velocity $(\omega_b/2\pi)(1/2)$ is found, although in this case only quasiperiodic MB's exist. For the sake of completeness we mention that the upper branch can be continued to lower values of the coupling and connects with MB's generated by the depinning mode, whereas the lower branch belongs to the spontaneous MB.

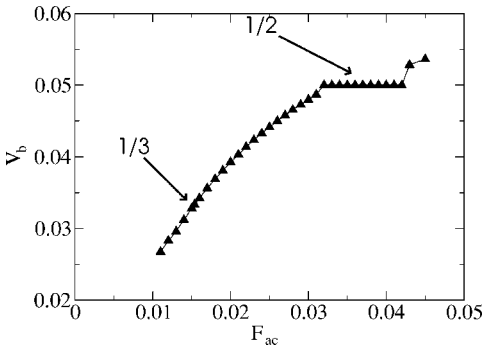

FIG. 3. Velocity of the MB vs F_{ac} showing two mode-locking plateaus ($\frac{1}{3}$ and $\frac{1}{2}$) for $C=0.75$, the values of γ and ω_b are the same that in Fig. 2.

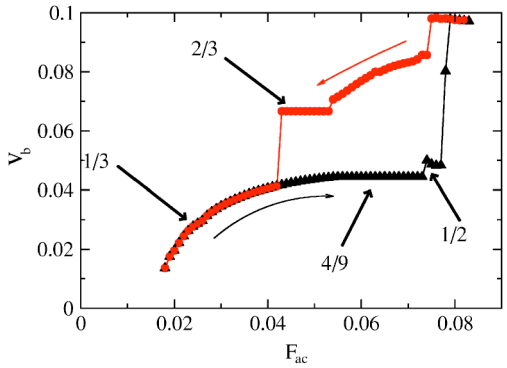

FIG. 4. (Color online) Same as Figs. 2 and 3 now for $C=0.94$. Several mode-locking steps are visible. Note also the hysteresis in the curve.

Summarizing, the step with velocity $(\omega_b/2\pi)(1/3)$ is found in all the range of coupling where MB's seem to exist. The range for the step solutions with $v_b=(\omega_b/2\pi)(1/2)$ starts at $C=0.71$ since below this coupling a MB with regular motion does not exist in the parameter range studied. At higher C, we observe other locking steps like $v_b=(\omega_b/2\pi)(4/9)$ and $v_b=(\omega_b/2\pi)(2/3)$ for $C=0.94$. Although we have not been exhaustive varying in the parameter C we can certainly find these steps (and others) in the whole range of coupling parameters, where DB's are found.

Some of the observed locking plateaus coincide with the stability interval of the corresponding (p/q)-resonant MB, but in other cases (notably the $1/2$ locking step shown in Fig. 3) the resonant state destabilizes inside the plateau and the new attracting solution (with locking velocity v_b) is more complex: either periodic with a larger period or even chaotic, as revealed by the computed (largest) Lyapunov exponent. These types of complex behaviors inside a locking plateau are known to happen for a single driven-damped anharmonic oscillator [20], as well as for moving discommensurations [21]. In this regard, the result for discommensurations can be reducible to the single-particle case using collective variable approaches. In our case, the breather internal degrees of freedom, together with the X (breather center) variable, do not allow for a straightforward reduction to single-particle behavior.

IV. UNLOCKING TRANSITION

A typical route for the transition from a periodic state to a quasiperiodic or chaotic one in dissipative systems is that mediated by intermittencies [22]. Intermittencies occur whenever the behavior of a system seems to switch between qualitatively different unstable periodic orbits or behaviors (periodic, quasiperiodic, or chaotic) even though all the control parameters remain constant and no external noise is present [23]. Depending on the type of Floquet instability of the periodic orbit responsible for the bifurcation (crossing the unit circle at +1, at two complex conjugate eigenvalues, or at −1) intermittencies are classified into intermittencies type I, II, or III, respectively [22].

In this section we study the unlocking transition of the (p/q)-resonant MB and characterize it as a transition from

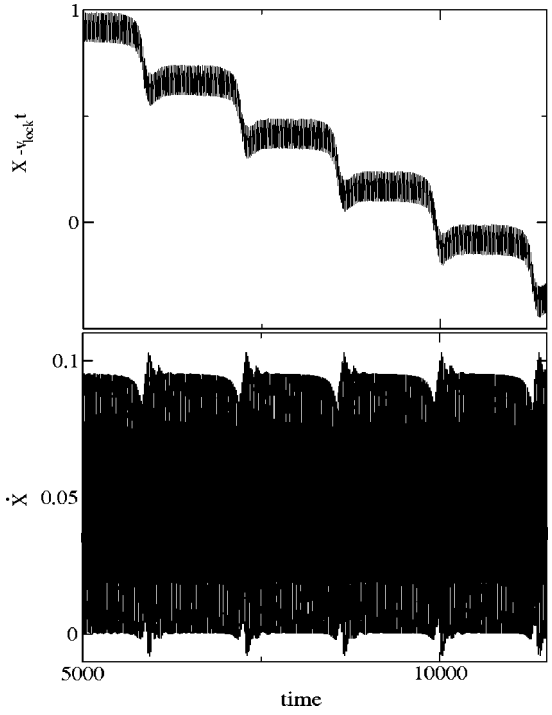

FIG. 5. Upper panel: $X-v_{lock}t$—i.e., X respect to a moving frame that moves with $v_b=(\omega_b/2\pi)1/2$ just below the left edge of the $\frac{1}{2}$ step of the Fig. 3. Jumps correspond to the intermittencies described in the text. Lower panel: $\dot{X}$ in the same point of response curve.

periodicity to quasiperiodicity driven by the regular (periodic) appearance of type-I intermittencies. This mechanism for unlocking transitions was already observed in the purely dissipative dynamics of ac-driven modulated structures of the FK model [24]. Intermittencies of type I are also known to be responsible for the depinning transition of discrete solitons (discommensurations) of the underdamped FK model [21].

From now on in this section we will focus our attention on the unlocking transition at the left edge of the $1/2$ locking step of Fig. 3 ($C=0.75$) which occurs at $F_{ac}=0.03177$. The extended Floquet analysis of the $(1/2)$-resonant MB close to the edge reveals that an eigenvalue of the Floquet matrix $D(\mathcal{L}T^2)$ approaches the value +1 from the interior of the complex unit circle along the real axis and leaves the unit circle at the transition point. The eigenvector associated with this Floquet eigenvalue is exponentially localized at the breather center. Out the step, the $(1/2)$-resonant MB is thus linearly unstable.

In order to visualize the effect of this instability we plot in Fig. 5 the breather center (out of the step but very close to its edge) X and its velocity $\dot{X}$ in a reference frame moving with the locking velocity $(\omega_b/2\pi)(1/2)$. One can clearly see in Fig. 5 that the breather center remains for some time intervals in laminar regimes (of locked velocity), interrupted by sudden jumps of very short duration.

We have numerically checked that these laminar regimes correspond to the discrete family of equivalent unstable continuations of the $(1/2)$-resonant MB, related one to each

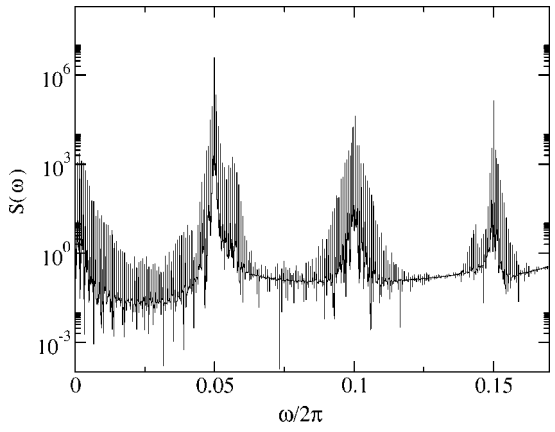

FIG. 6. Power spectrum $S(\omega)$ of $\dot{X}$ showing clearly a quasiperiodic behavior.

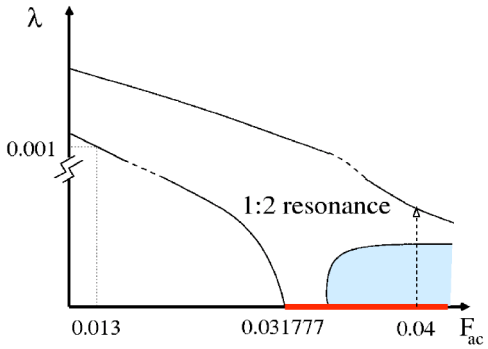

FIG. 7. (Color online) Schematic phase diagram of the behavior with a subharmonic perturbation of strength λ vs unperturbed driving force amplitude F_{ac}. The shaded region refers to more complex behavior (chaotic, quasiperiodic, or higher resonances than 1/2) but also mode locking. The arrow stands for the path followed in Fig. 8.

other by the symmetry operations $\mathcal{L}$, $\mathcal{S}$, and $\mathcal{T}$. Therefore, the destabilizing Floquet eigenvector pushes the weakly unstable resonant MB $\hat{u}$ towards its (equivalent) closest member of the family (which turns out to be $\mathcal{S}^{-1}\hat{u}$), which is also unstable, and so on. The duration of each laminar regime, which diverges at the bifurcation point, is proportional to $(\mu-1)^{-1}$, where μ is the unstable Floquet eigenvalue.

The computation of the *power spectrum* of $\dot{X}$, i.e.,

$$S(\omega) = \left| \int_{-\infty}^{\infty} \dot{X}(t) e^{i\omega t} dt \right|^2, \tag{12}$$

for the attracting MB out of the locking plateau (see Fig. 6), reveals the new frequency $\omega_{int}=\mu-1$ associated with the intermittencies and further confirms that they appear at regular time intervals, so that the attracting MB out of the step is quasiperiodic.

This scenario of the unlocking mechanism is confirmed to happen for other numerically obtained plateaus of the mode-locked velocity. It appears that the desynchronization by regular intermittent phase shift pulses is quite a generic phenomenon.

V. EFFECTS OF SUBHARMONIC PERTURBATIONS OF THE DRIVING FORCE

In the previous sections, we have shown how complex the dynamical response of the system can be. This includes, among others, resonant MB's which are destabilized via intermittencies when the parameters are changed. Inside the resonant step, the particular behavior of the oscillators forming the breather can be complex (high order periodic or chaotic). However, it does not prevent the breather from having a definite mean velocity, commensurate with the external frequency.

Our goal in this section is to enlarge the regions of the parameter space for which those resonant steps exist. The structure of the quasiperiodic attractor in the vicinity of the resonant steps gave us some indications about the procedure to follow. We must reinforce the laminar phase (correspondingly inhibit the appearance of intermittencies), applying a perturbation subharmonically related with the original ac force:

$$F(t) = F_{ac}\sin(\omega_b t) + \lambda \sin\left(\frac{\omega_b}{n}t + \Delta\right), \tag{13}$$

where λ is small compared to F_{ac}, n is a positive integer, and Δ represents a phase shift between both terms.

Such a kind of perturbation has been proven to be efficient to stabilize linearly unstable periodic orbits. It has been used in systems with a few degrees of freedom [25,26] as well as in solitons [27] and even in experiments [28]. In our case we achieve lowering the onset of the resonant steps significantly. In particular, we focus our attention on the step 1/2 in $C=0.75$ which presents the richest phenomenology, and choose $n=2$ in Eq. (13) and $\Delta=0$ (other Δ values have been used and the results obtained are essentially similar). The main results are summarized in the phase diagram of Fig. 7. For example, the onset of the resonant step is reduced from $F_{ac}=0.031\,777$ to $F_{ac}\simeq 0.013$ when λ increases from 0 to $\lambda\simeq 0.001$.

This effect adds to another that takes place inside the step and that is related to the control of chaos. A chaotic attractor like the one developed by a period-doubling cascade inside the 1/2-resonant step for values $F_{ac}\approx 0.038\,33$ (with $\lambda=0$) is formed by a dense set of unstable periodic orbits of different periodicities but all of the same velocity. The addition of a suitable perturbation is able to stabilize one of these unstable periodic orbits. The taming of chaotic states in nonantonomous dynamical systems by the addition of harmonic perturbations is a quite general phenomenon [25,27,29], and we observe it in the case of these chaotic breathers with locked velocity.

To quantify this behavior we compute the largest Lyapunov exponent [30] of the MB solution at a fixed $F_{ac}=0.04$ as a function as the perturbation strength λ. We start at a chaotic mode-locking MB. As soon as we apply the perturbation, a significant decrease of the largest Lyapunov exponent is observed until a narrow region of quasiperiodicity is reached (largest Lyapunov exponent=0). Then, a sequence of periodic and quasiperiodic solutions follows and, finally, a

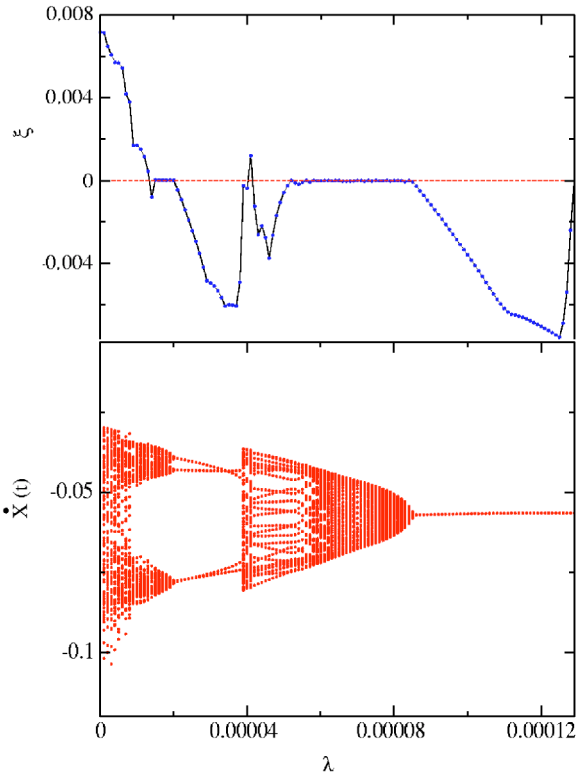

FIG. 8. (Color online) (Upper) Largest Lyapunov exponent (ξ) for $F_{ac}=0.04$. (Lower) Poincaré section of X at intervals $2T_b$, so a single point is indicative of a periodic solution in the mode-locking step at its corresponding λ value.

broad region of periodic solution, with the perturbation period (see Fig. 8). Note that all this is attained with a λ two orders of magnitude smaller than F_{ac}.

At fixed C, one can *tune*, by varying λ, the desired periodic state. This method is extremely robust against changes in C. The pure resonant MB solution can be extended for a wide range of the coupling C. Using an appropriated λ we have extended the $1/2$-resonant solution from [0.71, 0.84] to [0.5, 0.84] in the coupling parameter.

VI. CONCLUDING REMARKS AND SUMMARY

We have studied mobile discrete breathers in the underdamped Frenkel-Kontorova model. Periodic (or p/q-resonant) solutions have been found for a large range of parameter values (as C and F_{ac}). These states are structurally stable as they are a consequence of the synchronization between the two time scales of the mobile breather. This synchronization (or its absence) results in a very rich dynamics of the mobile breather solutions, including quasiperiodic and chaotic ones. Localized chaotic behavior has been previously observed in static breathers [31], but here we show that it is compatible with the mode-locking motion of the breather center (core).

One important issue in the study of localized discrete excitations is the possibility of their dynamical description by reduction to a system with few degrees of freedom (or collective coordinates). To our knowledge, two collective coordinate schemes have been developed with mobile breathers. The first approach described in [32] has produced very fruitful results for discrete [21] and continuum [33] solitons, as well as for continuum breathers [34,35]. This approach uses as a starting point for the calculations the continuum model solution and fails far from this limit.

The second approach [36] is the geometric counterpart of the first. It works with mobile breathers in a Hamiltonian framework, which prevents its direct use in the dissipative case considered here. However, the possibility of its use in non-Hamiltonian contexts, under certain technical conditions, is still open as was briefly pointed out in Ref. [37].

Although analytical methods for a collective coordinate approach to mobile dissipative discrete breathers have not been yet developed, our numerical results strongly suggest that such an approach could give an accurate account of most of the observed phenomenology. We hope that the results presented here could encourage a search of those methods.

Finally, we remark on the important role that a second harmonic in the forcing plays in the dynamics of the MB. We observe that the presence of a small subharmonic driving term enhances (p/q)-resonant solutions. Increasing the subharmonic amplitude (13) from zero, an initially chaotic MB can be tamed, above some threshold, obtaining a nonchaotic one [quasiperiodic or (p/q) resonant]. The feasibility of the experimental implementation of different wave forms for driving forces could falicitate the observation of these solutions since they are more robust and stable.

In summary, we have shown that the mode-locking motions of breathers are stable solutions for an important example of nonlinear lattices such as the Frenkel-Kontorova model. We have characterized this mode-locking solution as well as the mechanisms for the unlocking. Finally we have applied a simple method to extend this kind of solutions to a large range of values in parameter space.

ACKNOWLEDGMENTS

We thank J. L. García Palacios and J. J. Mazo for a reading of the manuscript. D.Z. is grateful to M. Meister for discussions. Financial support from European Network LOCNET Grant No. HPRN-CT-1999-00163 and also from the Spanish MCyT and European Regional Development Fund (FEDER) program through the BFM2002-00113 project is acknowledged.

[1] A. C. Scott, *Nonlinear Science: Emergence and Dynamics of Coherent Structures* (Oxford University Press, Oxford, 1999).
[2] S. Flach and C. R. Willis, Phys. Rep. **295**, 181 (1998).
[3] G. P. Tsironis, M. Ibañes, and J. M. Sancho, Europhys. Lett. **57**, 697 (2002).
[4] A. R. McGurn, Chaos **13**, 754 (2003) and references therein.
[5] E. Trias, J. J. Mazo, and T. P. Orlando, Phys. Rev. Lett. **84**, 741 (2000).
[6] P. Binder, D. Abraimov, A. V. Ustinov, S. Flach, and Y. Zolotaryuk, Phys. Rev. Lett. **84**, 745 (2000).
[7] F. S. Cataliotti, S. Burger, C. Fort, P. Maddaloni, F. Minardi, A. Trombettoni, A. Smerzi, and M. Inguscio, Science **293**, 843 (2001).
[8] M. Eleftheriou and G. P. Tsironis, Phys. Scr. **71**, 318 (2005).
[9] L. M. Floría and P. J. Martínez, in *Nonlinear Encyclopedia*, edited by A. C. Scott (Routledge, New York, 2005), p. 336–339.
[10] O. M. Braun and Y. S. Kivshar, Phys. Rep. **306**, 1 (1998).
[11] L. M. Floría and J. J. Mazo, Adv. Phys. **45**, 505 (1996).
[12] P. J. Martínez, M. Meister, L. M. Floría, and F. Falo, Chaos **13**, 610 (2003).
[13] R. S. Mackay and J. A. Sepulchre, Physica D **119**, 148 (1998).
[14] Y. S. Kivshar and S. Flach, Chaos **13**, 586 (2003).
[15] J. L. Marín, F. Falo, P. J. Martínez, and L. M. Floría, Phys. Rev. E **63**, 066603 (2001).
[16] D. Chen, S. Aubry, and G. P. Tsironis, Phys. Rev. Lett. **77**, 4776 (1996).
[17] S. Aubry and T. Cretegny, Physica D **119**, 34 (1998).
[18] N. R. Quintero and A. Sánchez, Eur. Phys. J. B **6**, 133 (1998).
[19] M. Meister (private communication).
[20] G. L. Baker and J. P. Gollub, *Chaotic Dynamics: An Introduction* (Cambridge University Press, Cambridge, England, 1996).
[21] P. J. Martínez, F. Falo, J. J. Mazo, L. M. Floría, and A. Sánchez, Phys. Rev. B **56**, 87 (1997).
[22] F. Bergé, Y. Pomeau and Ch. Vidal, *Order within Chaos* (Wiley, New York, 1984).
[23] R. C. Hilborn, *Chaos and Nonlinear Dynamics* (Oxford University Press, Oxford 1994).
[24] F. Falo, L. M. Floría, P. J. Martínez, and J. J. Mazo, Phys. Rev. B **48**, 7434 (1993).
[25] Y. Braiman and I. Goldhirsch, Phys. Rev. Lett. **66**, 2545 (1991).
[26] M. Barbi and M. Salerno, Phys. Rev. E **63**, 066212 (2001).
[27] M. Salerno, Phys. Rev. B **44**, 2720 (1991).
[28] S. T. Vohra, L. Fabiny, and F. Bucholtz, Phys. Rev. Lett. **75**, 65 (1995).
[29] R. Chacón and J. A. Martínez, Phys. Rev. E **65**, 036213 (2002).
[30] H. G. Schuster, *Deterministic Chaos: An Introduction* (VCH, Weinheim, (1988).
[31] P. J. Martínez, L. M. Floría, F. Falo, and J. J. Mazo, Europhys. Lett. **45**, 444 (1999).
[32] C. Willis, M. El-Batanouny, and P. Stancioff, Phys. Rev. B **33**, 1904 (1986).
[33] L. Morales-Molina, N. R. Quintero, F. G. Mertens, and A. Sánchez, Phys. Rev. Lett. **91**, 234102 (2003).
[34] A. Sánchez and A. R. Bishop, SIAM Rev. **40**, 579 (1998).
[35] J. G. Caputo and N. Flytzanis, Phys. Rev. A **44**, 6219 (1991).
[36] R. S. Mackay and J. A. Sepulchre, J. Phys. A **35**, 3985 (2002).
[37] R. S. Mackay, in *Energy Localization and Transfer*, edited by T. Dauxois *et al.* (World Scientific, Singapore, 2004), pp. 149–192.